J. Chem. Eng. Data **1995,** *40,* 153–159

Vapor–Liquid Equilibria for Hydrogen Sulfide + Hexane, + Cyclohexane, + Benzene, + Pentadecane, and + (Hexane + Pentadecane)

Serge Laugier

Ecole Nationale Supérieure de Chimie et Physique de Bordeaux, UA503 LPCT-Equipe IAGP,
351 Cours de la Libération, 33405 Talence, France

Dominique Richon*

Laboratoire de Thermodynamique, Centre Réacteurs et Processus, Ecole Nationale Supérieure des Mines de
Paris, 35 rue Saint-Honoré, 77305 Fontainebleau, France

A static-based apparatus with capillary sampling has been used to measure vapor–liquid equilibria up to 11.2 MPa at three temperatures around 323, 373, and 423 K for the following systems: hydrogen sulfide + hexane, + cyclohexane, + benzene, + pentadecane, and + (hexane + pentadecane).

Introduction

Many petroleum reservoirs contain hydrogen sulfide as a constituent, and in most cases its presence has been taken into account for multicomponent phase equilibria modeling. It is, however, not easy to make accurate calculations when H_2S is a component because of the lack of vapor–liquid equilibrium (VLE) data for either binary or ternary mixtures involving this compound. Results presented here were used to test thermodynamic models for predicting binary and multicomponent phase equilibria.

Experimental Section

Apparatus and Procedure. The apparatus used in this work is based on the static method with sampling of both phases. It has been described in previous papers (*1*, *2*). Due to the corrosive character of the hydrogen sulfide, the capillary sampling technique (*3*) appeared as the most suitable. Some improvements were however necessary. The whole apparatus was settled inside a huge fumehood, and all H_2S-containing exhausts were bubbled inside a soda aqueous solution. The flow diagram of the apparatus is given in Figure 1.

The pressure membrane transducer was replaced by a homemade null pressure transducer. This transducer is composed of a bellows separating the mixture from a pressurizing gas (nitrogen). The nitrogen side of the bellows holds a rod, the extremity of which is magnetic. This magnetic extremity moves against an outside Hall effect proximity sensor connected to a multimeter. The multimeter is able to monitor the electrovalves when selected electromotive force (emf) values are reached. The two limiting emf values are chosen very close to obtain the maximum null pressure sensitivity and then accurately measure the equilibrium cell internal pressure through the digital Bourdon manometer (BM), working with nitrogen at room temperature. Metals in contact with mixtures are either 316L stainless steel or monel (capillaries).

Liquid (LI) and vapor (VI) injectors are heated using heating resistances. They can withstand temperatures up to 580 K, but at this temperature hydrogen sulfide reacts significantly with stainless steel. It was then decided to keep the injectors at a temperature around 420 K. This temperature is however not high enough to quickly vaporize liquid samples containing pentadecane. For this reason, a special device, TFVB, was introduced in the chromatographic circuit after passing inside the injectors and before returning to the chromatograph. This trap–flash vaporization bath has two roles: trapping and vaporizing. It can contain either a refrigerating or a high-temperature liquid. When a sample is taken through the liquid injector, the hydrogen sulfide flows through the cold coil immersed in the cold TFVB bath up to the chromatograph detector (thermal conductivity detector) while pentadecane is condensed (enough time is allowed to transfer all pentadecane from injector to the cold coil, generally less than 1/2 h). Then by using a high-temperature liquid salt (around 600 K) in the TFVB, the pentadecane is instantaneously vaporized to normal chromatographic conditions. For all mixtures not containing pentadecane the special TFVB device was removed.

Table 1. Origin and Purity of Chemicals

component	origin	purity by GLC/(mol %)
hydrogen sulfide	Air Liquide	99.999
benzene	Merck	99.7
cyclohexane	Merck	99.7
hexane	Merck	99.0
pentadecane	Merck	99.0

The experimental procedure is as described by Laugier et al. (*3*), except for pressure determinations and analyses using the TFVB device. The sources and purities of the chemicals are listed in Table 1.

Uncertainties in pressures result from calibration of the digital Bourdon manometer connected to the null pressure transmitter. They are reported in Tables 2–6. Temperature measurements are carried out using platinum probes (PP) calibrated against a reference platinum probe. Estimated temperature uncertainties δT are also reported in Tables 2–6.

Vapor-phase (y) and liquid-phase (x) mole fractions were obtained through GLC determinations. The thermal conductivity detector is equipped with a platinum wire for corrosion purposes. Its calibration was carried out by injecting known amounts of pure components. The uncertainties reported in Tables 2–6 take into account the

0021-9568/95/1740-0153$09.00/0

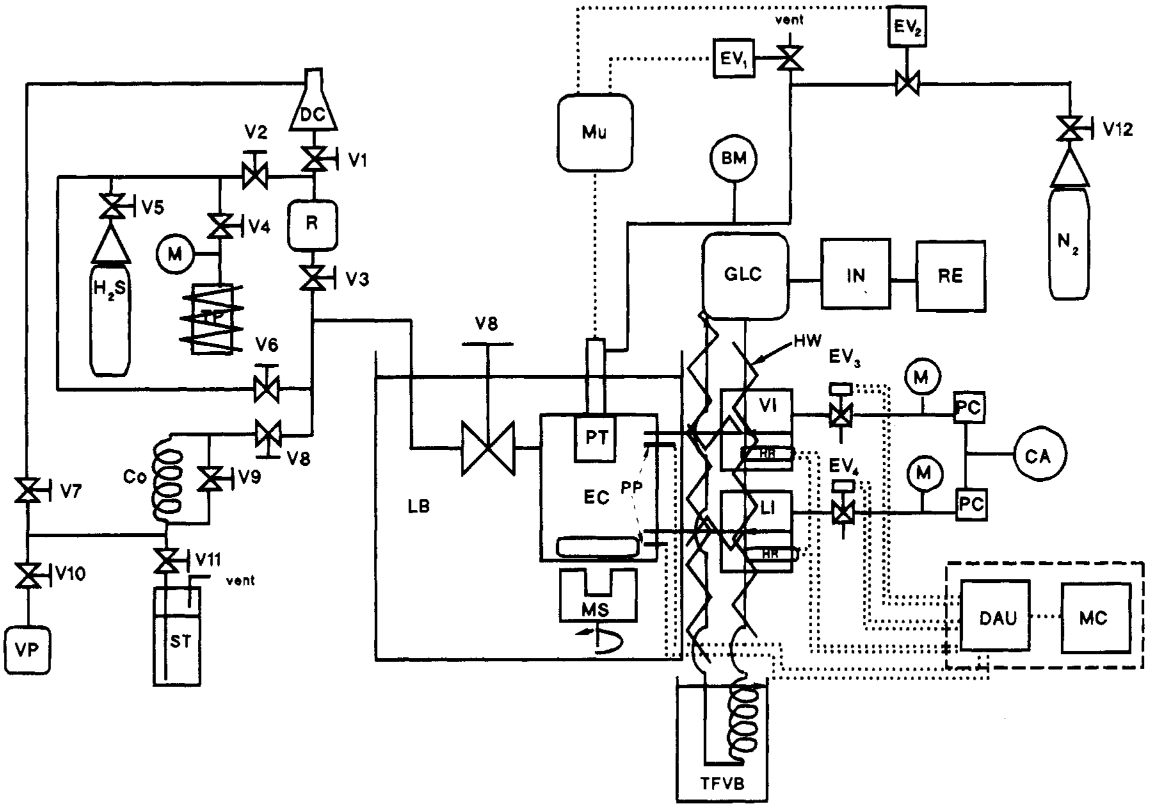

Figure 1. Key: BM, Bourdon manometer; CA, compressed air; Co, coil; DAU, data acquisition unit; DC, degassing cell; EC, equilibrium cell; EV, electrovalve; GLC, gas–liquid chromatograph; HR, heating resistance; HW, heating wire; IN, integrator; LB, liquid bath; LI, liquid injector; M, manometer; MC, microcomputer; MS, magnetic stirrer; Mu, multimeter; PC, pressurizing circuit; PP, platinum probe; PT, pressure transducer; R, reservoir; RE, recorder; ST, soda trap; TFVB, trap–flash vaporization bath; TP, thermal press; V, shut-off valve; VI, vapor injector; VP, vacuum pump.

Table 2. Vapor–Liquid Equilibrium at Temperature *T*, Pressure *P*, and Liquid Phase x_1 and Vapor Phase y_1 Mole Fractions for Hydrogen Sulfide (1) + Hexane(2)

T/K	P/MPa[c]	x_1	$10^3\delta x_1$	y_1	$10^3\delta y_1$	P_{cal}/MPa[d]	$y_{1,cal}$[d]
322.9_5[a]	0.430	0.095	3	0.871	5	0.410	0.8684
322.9_5[a]	0.840	0.199	5	0.935	2	0.804	0.9326
322.9_5[a]	1.205	0.307	6	0.955	2	1.211	0.9555
322.9_5[a]	1.600	0.421	6	0.969	2	1.635	0.9676
322.9_5[a]	2.000	0.539	6	0.976_0	1	2.059	0.9754
322.9_5[a]	2.380	0.656	5	0.981_0	1	2.457	0.9809
322.9_5[a]	2.790	0.788	4	0.986_5	0.7	2.873	0.9863
322.9_5[a]	3.200	0.914	2	0.987_4	1	3.248	0.9922
372.9_5[b]	0.985	0.114	3	0.743	6	0.988	0.7340
372.9_5[b]	1.835	0.237	5	0.851	3	1.826	0.8483
372.9_5[b]	2.745	0.367	6	0.900	4	2.753	0.8941
372.9_5[b]	3.665	0.485	6	0.921	4	3.631	0.9162
372.9_5[b]	4.480	0.590	6	0.935	3	4.446	0.9295
372.9_5[b]	5.360	0.692	6	0.945	3	5.277	0.9397
372.9_5[b]	6.360	0.792	5	0.955	2	6.161	0.9492
372.9_5[b]	7.390	0.900	3	0.970	2	7.302	0.9630
422.6_5[b]	0.910	0.023_0	0.8	0.184	4	0.951	0.1884
422.6_5[b]	1.190	0.056	2	0.366	6	1.248	0.3583
422.6_5[b]	1.995	0.144	3	0.584	7	2.062	0.5810
422.6_5[b]	2.810	0.232	4	0.687	6	2.912	0.6822
422.6_5[b]	3.595	0.301	5	0.741	6	3.605	0.7289
422.6_5[b]	4.575	0.395	7	0.781	5	4.585	0.7693
422.6_5[b]	5.500	0.481	7	0.808	4	5.517	0.7922
422.6_5[b]	6.385	0.551	7	0.825	4	6.296	0.8036
422.6_5[b]	7.545	0.637	6	0.825	3	7.256	0.8090

[a] δT = 0.1 K. [b] δT = 0.2 K. [c] δP = 0.005 MPa. [d] Calculated values with the RKS equation of state and R1 rule (binary parameter given in Table 8).

uncertainty on detector calibration, and the reproducibility of the chromatographic ratio areas on at least five samples, corresponding to the same equilibrium.

Table 3. Vapor–Liquid Equilibrium at Temperature *T*, Pressure *P*, and Liquid Phase x_1 and Vapor Phase y_1 Mole Fractions for Hydrogen Sulfide (1) + Cyclohexane (2)

T/K	P/MPa[c]	x_1	$10^3\delta x_1$	y_1	$10^3\delta y_1$	P_{cal}/MPa[d]	$y_{1,cal}$[d]
323.0_5[a]	0.400	0.085	3	0.890	3	0.407	0.9108
323.0_5[a]	0.665	0.142	3	0.942	2	0.651	0.9441
323.0_5[a]	1.075	0.252	5	0.964	2	1.110	0.9671
323.0_5[a]	1.420	0.330	5	0.972_7	1	1.420	0.9744
323.0_5[a]	1.780	0.414	6	0.978_9	1	1.738	0.9794
323.0_5[a]	2.190	0.533	7	0.982_9	0.6	2.150	0.9840
323.0_5[a]	2.585	0.657	6	0.986_0	1	2.527	0.9873
323.0_5[a]	3.035	0.776	5	0.989_5	0.5	2.849	0.9902
372.5_5[b]	1.150	0.135	3	0.835	5	1.154	0.8418
372.5_5[b]	1.970	0.245	5	0.904	3	1.975	0.9035
372.5_5[b]	2.745	0.352	6	0.931	3	2.786	0.9288
372.5_5[b]	3.630	0.480	6	0.952	3	3.767	0.9452
372.5_5[b]	4.630	0.605	6	0.957	2	4.733	0.9551
372.5_5[b]	5.345	0.692	6	0.961	1	5.416	0.9606
372.5_5[b]	6.305	0.806	4	0.967	2	6.364	0.9677
372.5_5[b]	7.190	0.890	3	0.976	1	7.178	0.9746
422.6_5[b]	1.085	0.0544	1	0.477	6	1.097	0.4726
422.6_5[b]	2.425	0.184	4	0.740	5	2.463	0.7424
422.6_5[b]	3.625	0.283	5	0.815	4	3.562	0.8091
422.6_5[b]	4.820	0.391	5	0.851	3	4.819	0.8470
422.6_5[b]	6.000	0.477	6	0.872	3	5.865	0.8649
422.6_5[b]	7.180	0.575	6	0.882	3	7.106	0.8774
422.6_5[b]	8.430	0.653	6	0.890	3	8.130	0.8826
422.6_5[b]	9.495	0.724	5	0.890	3	9.075	0.8829

[a] δT = 0.1 K. [b] δT = 0.2 K. [c] δP = 0.005 MPa. [d] Calculated values with the RKS equation of state and R1T rule (binary parameter given in Table 8).

Experimental Results

P, *T*, *x*, and *y* results are reported in Tables 2–5 for binary mixtures and Table 6 for the ternary mixture. Each

Table 4. Vapor–Liquid Equilibrium at Temperature T, Pressure P, and Liquid Phase x_1 and Vapor Phase y_1 Mole Fractions for Hydrogen Sulfide (1) + Benzene (2)

T/K	P/MPa[c]	x_1	$10^3\delta x_1$	y_1	$10^3\delta y_1$	P_{cal}/MPa[d]	$y_{1,cal}$[d]
323.1_5[a]	0.455	0.144	3	0.919	2	0.445	0.9231
323.1_5[a]	0.790	0.262	5	0.954	2	0.798	0.9592
323.1_5[a]	1.220	0.398	6	0.973_0	1	1.225	0.9755
323.1_5[a]	1.615	0.521	6	0.981_2	0.7	1.635	0.9834
323.1_5[a]	2.010	0.626	6	0.986_0	0.5	2.004	0.9881
323.1_5[a]	2.415	0.738	4	0.990_3	0.4	2.422	0.9920
323.1_5[a]	2.795	0.831	3	0.993_2	0.6	2.794	0.9949
323.1_5[a]	3.230	0.936	2	0.996_6	0.3	3.252	0.9980
372.6_5[a]	0.930	0.129	3	0.779	4	0.925	0.8066
372.6_5[a]	1.830	0.275	5	0.886	3	1.840	0.9025
372.6_5[a]	2.720	0.408	6	0.925	3	2.749	0.9351
372.6_5[a]	3.660	0.530	7	0.949	2	3.661	0.9521
372.6_5[a]	4.480	0.633	6	0.957_3	1	4.503	0.9622
372.6_5[a]	5.420	0.737	5	0.967_2	1	5.442	0.9705
372.6_5[a]	6.290	0.818	4	0.973_2	0.9	6.258	0.9765
372.6_5[a]	7.155	0.897	3	0.980_6	0.8	7.164	0.9828
422.6_5[b]	1.100	0.055_9	1	0.437	7	1.091	0.4531
422.6_5[b]	2.330	0.175	3	0.703	7	2.252	0.7204
422.6_5[b]	3.510	0.300	6	0.806	5	3.573	0.8139
422.6_5[b]	4.725	0.400	7	0.847	3	4.718	0.8521
422.6_5[b]	6.075	0.508	6	0.875	3	6.058	0.8776
422.6_5[b]	7.460	0.599	6	0.892	2	7.282	0.8916
422.6_5[b]	8.715	0.680	5	0.899	2	8.451	0.8995
422.6_5[b]	9.800	0.746	5	0.902	2	9.452	0.9024

[a] $\delta T = 0.1$ K. [b] $\delta T = 0.2$ K. [c] $\delta P = 0.005$ MPa. [d] Calculated values with the RKS equation of state and R1 rule (binary parameter given in Table 8).

Table 5. Vapor–Liquid Equilibrium at Temperature T, Pressure P, and Liquid Phase x_1 and Vapor Phase y_1 Mole Fractions for Hydrogen Sulfide (1) + Pentadecane (2)

T/K[a]	P/MPa[b]	x_1	$10^3\delta x_1$	y_1	$10^3\delta y_1$	P_{cal}/MPa[c]	$y_{1,cal}$[c]
422.6	1.13	0.167	5	0.9980	0.6	1.13	0.9972
422.6	2.39	0.303	7	0.9987	0.5	2.34	0.9982
422.6	4.45	0.484	10	0.9987	1	4.45	0.9983
422.6	6.03	0.601	10	0.9986	0.7	6.18	0.9980
422.6	7.38	0.680	9	0.9987	0.9	7.54	0.9975
422.6	9.10	0.761	8	0.9975	0.6	9.10	0.9965
422.6	10.44	0.817	7	0.9971	0.6	10.28	0.9951
422.6	11.21	0.843	7	0.9960	0.7	10.85	0.9942

[a] $\delta T = 0.3$ K. [b] $\delta P = 0.01$ MPa. [c] Calculated values with the RKS equation of state and R2 rule (binary parameter given in Table 8).

table includes the uncertainty δ on each measured quantity. P, T, x, and y are shown for all mixtures in Figures 2–5.

Data Treatment

Two equations of state have been used for modeling purposes: the Redlich–Kwong–Soave equation of state (RKS-EoS) (*4*) and the Peng–Robinson equation of state (PR-EoS) (*5*). These equations presented in the Appendix were used with different mixing and combining rules. The values of the pure component characteristic properties (*6*) are given in Table 7.

For mixing and combining rules R1 and R2, binary interaction parameters have been adjusted on experimental data by minimizing the following objective function

$$Q = \sum_{j=1}^{n} \{[(P_{j,\mathrm{exp}} - P_{j,\mathrm{cal}})/P_{j,\mathrm{exp}}]^2 + [(y_{j,\mathrm{exp}} - y_{j,\mathrm{cal}})/y_{j,\mathrm{exp}}]^2\} \tag{1}$$

with temperature (T) and liquid mole fraction (x) chosen as independent variables. P is the total pressure and y, the vapor mole fraction.

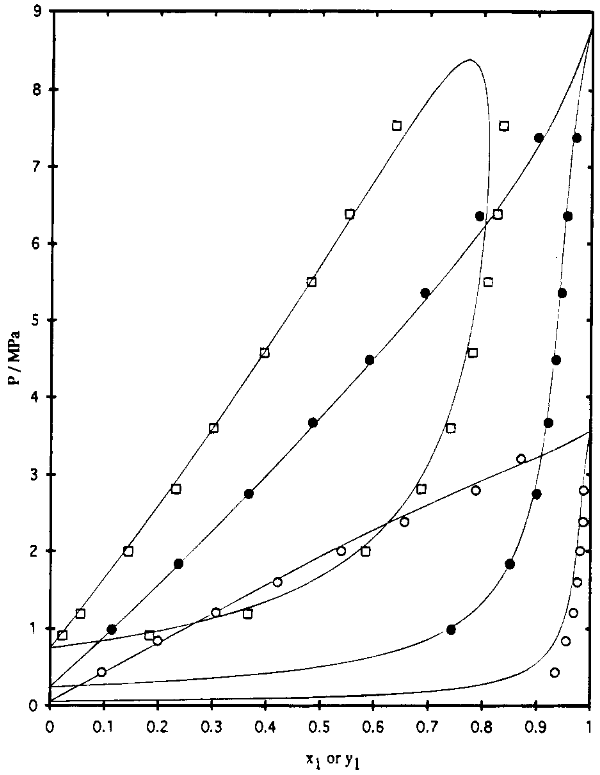

Figure 2. Pressure as a function of hydrogen sulfide mole fraction in the hydrogen sulfide (1) + hexane (2) system at different temperatures: 323 K (○); 373 K (●); 423 K (□); (—) calculated results with the RKS-EoS and binary interaction parameter (R1 rule) given in Table 8.

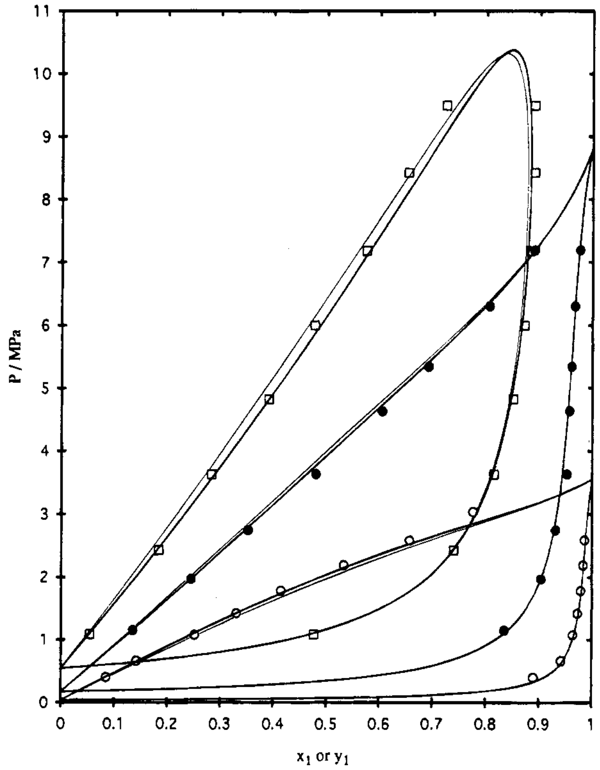

Figure 3. Pressure as a function of hydrogen sulfide mole fraction in the hydrogen sulfide (1) + cyclohexane (2) system at different temperatures: 323 K (○); 373 K (●); 423 K (□); (light line) calculated results with the RKS-EoS and binary interaction parameter (R1 rule) given in Table 8; (dark line) calculated results with the RKS-EoS and binary interaction parameters (R1T rule) given in Table 8.

Table 6. Vapor–Liquid Equilibrium at Temperature T, Pressure P, and Liquid Phase x_1 and x_2 and Vapor Phase y_1, y_2, and y_3 Mole Fractions for Hydrogen Sulfide (1) + Hexane (2) + Pentadecane (3)

T/K[a]	P/MPa[b]	x_1	$10^3\delta x_1$	x_2	$10^3\delta x_2$	y_1	$10^3\delta y_1$	y_2	$10^3\delta y_2$	y_3	$10^3\delta y_3$	P_{cal}/MPa[c]	$y_{1,cal}$[c]	$y_{2,cal}$[c]
424.5	1.23	0.063	3	0.880	5							1.279	0.3984	0.6012
424.5	1.21_5	0.068	3	0.860	5							1.307	0.4221	0.5775
424.5	1.22_5	0.073	3	0.855	5	0.436	8	0.564	8	0.0003	0.1	1.352	0.4393	0.5603
424.5	1.22	0.070	3	0.854	6	0.433	8	0.567	8	0.0005	0.1	1.321	0.4306	0.5690
424.5	1.51	0.096	4	0.883	5	0.482	8	0.518	8	0.0002	0.1	1.622	0.4860	0.5139
424.5	1.50_5	0.094	4	0.855	5	0.502	7	0.498	7	0.0003	0.1	1.568	0.4930	0.5067
424.5	1.53	0.099	4	0.844	5	0.513	8	0.486	8	0.0003	0.1	1.607	0.5081	0.4916
424.5	1.60	0.109	4	0.843	5	0.530	8	0.470	8	0.0002	0.1	1.710	0.5279	0.4718
424.5	3.00	0.254	7	0.728	8							3.155	0.7014	0.2985
424.5	3.05	0.255	7	0.722	8	0.720	6	0.280	6	0.0001	0.1	3.158	0.7046	0.2953
424.5	3.025	0.264	7	0.670	8	0.749	6	0.251	6	0.0003	0.1	3.184	0.7311	0.2685
424.5	4.63	0.398	9	0.592	9							4.671	0.7705	0.2294
424.5	4.51	0.402	9	0.581	9	0.791	6	0.209	6	0.0002	0.1	4.710	0.7763	0.2235
424.5	4.58_5	0.407	9	0.555	9	0.809	5	0.191	5	0.0003	0.1	4.743	0.7903	0.2093
424.5	4.52_5	0.405	9	0.535	9	0.823	5	0.176	5	0.0004	0.1	4.686	0.8012	0.1982
424.5	4.52_5	0.412	9	0.528	9							4.764	0.8038	0.1956
424.5	6.16	0.523	9	0.451	9	0.822	4	0.178	4	0.0003	0.2	6.089	0.8159	0.1835
424.5	6.08	0.537	9	0.420	9	0.848	5	0.151	4	0.0006	0.2	6.251	0.8314	0.1677
424.5	7.53	0.640	8	0.340	8	0.843	4	0.156	4	0.0006	0.2	7.531	0.8316	0.1673
424.5	7.45	0.637	8	0.329	8	0.869	4	0.130	4	0.0007	0.2	7.530	0.8460	0.1525
424.5	7.52	0.635	8	0.320	8							7.508	0.8555	0.1428

[a] $\delta T = 0.3$ K. [b] $\delta P = 0.01$ MPa. [c] Calculated values with the RKS equation of state and R2 rule (binary parameter given in Table 8).

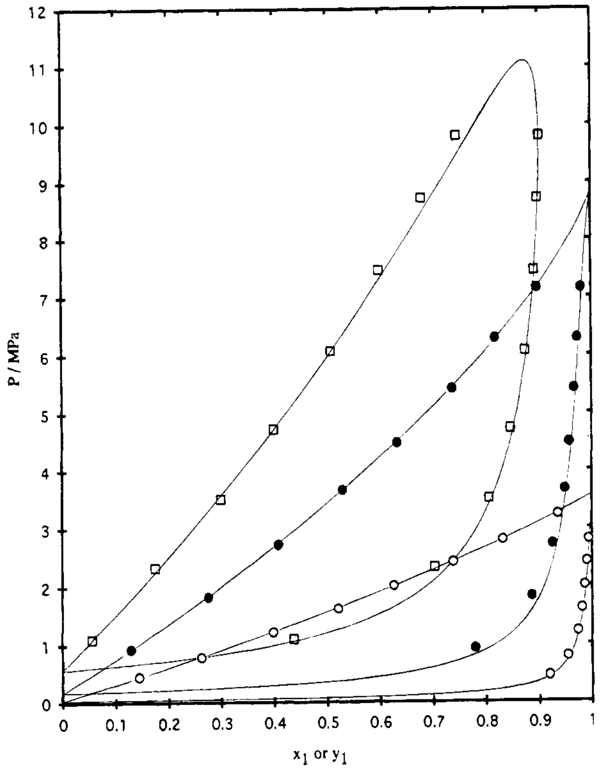

Figure 4. Pressure as a function of hydrogen sulfide mole fraction in the hydrogen sulfide (1) + benzene (2) system at different temperatures: 323 K (○); 373 K (●); 423 K (□); (—) calculated results with the RKS-EoS and binary interaction parameter (R1 rule) given in Table 8.

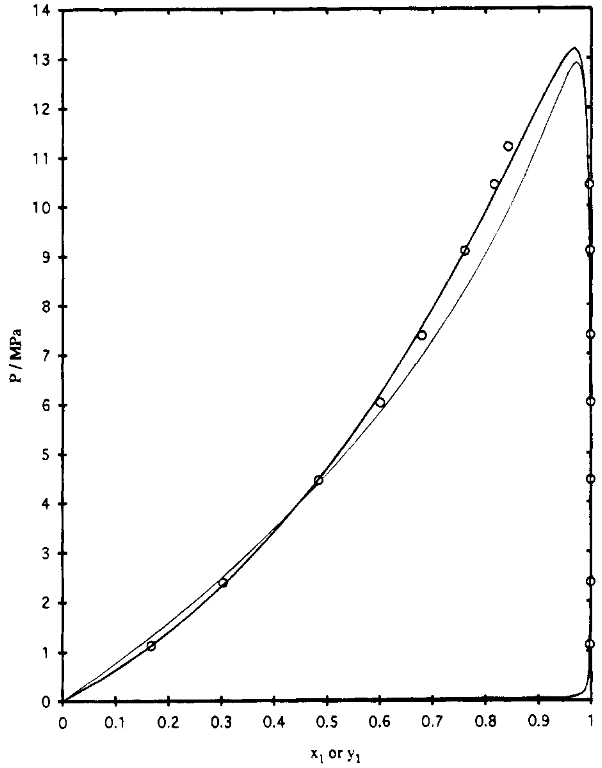

Figure 5. Pressure as a function of hydrogen sulfide mole fraction in the hydrogen sulfide (1) + pentadecane (2) system at 423 K (○); (light line) calculated results with the RKS-EoS (R0 rule); (dark line) calculated results with the RKS-EoS and binary interaction parameters (R2 rule) given in Table 8.

Table 7. Critical Parameters P_c and T_c and Acentric Factors ω Used in the Cubic Equations of State (Data Taken from Reference 6)

component	P_c/MPa	T_c/K	ω
hydrogen sulfide	8.940	373.2	0.100
benzene	4.898	562.2	0.212
cyclohexane	4.070	553.4	0.213
hexane	2.969	507.4	0.296
pentadecane	1.520	707.0	0.706

A representation of experimental data is summarized in Table 8. We may note that PR-Eos and RKS-Eos behave very similarly. For benzene + hydrogen sulfide the adjusted binary interaction parameter is very small. For hexane + hydrogen sulfide using mixing and combining rule R1 improves the pressure representation by a factor 4 as well as for cyclohexane + hydrogen sulfide. For the last mixture, a temperature-dependent binary interaction parameter for the a term leads to an improvement in the representation by a factor of 2. For pentadecane + hydrogen sulfide, the rules R1 and R0 are quite equivalent, while adjusting a binary interaction parameter on the b term (rule R2) is very efficient (improvement by a factor of 5 in the pressure representation).

Table 8. Representation of Vapor–Liquid Equilibrium Data of Mixtures Using Cubic Equations of State[a]

			PR-EoS			RKS-EoS		
binary mixture	number of binary data	mixing and combining rule	values of adjusted parameters	σ^R_p/%	σ^R_y/%	values of adjusted parameters	σ^R_p/%	σ^R_y/%
hydrogen sulfide (1) + benzene (2)	24	R0		2.0	1.1		1.9	1.2
		R1(δ_{12})	0.004	1.5	1.3	0.004	1.5	1.3
hydrogen sulfide (1) + cyclohexane (2)	24	R0		20.	2.3		20.	2.4
		R1(δ_{12})	0.073	4.6	1.2	0.078	4.3	1.0
		R1T(δ_{12},δ'_{12})	0.151, −0.347	2.5	1.3	0.197, −0.337	2.5	0.7
hydrogen sulfide (1) + hexane (2)	25	R0		13.	3.5		14.	4.0
		R1(δ_{12})	0.060	2.7	1.8	0.070	2.6	1.2
hydrogen sulfide (1) + pentadecane (2)	8	R0		11.	0.3		9.6	0.1
		R1(δ_{12})	−0.016	10.	0.2	0.000	9.6	0.1
		R2($\delta_{a_{12}}$,$\delta_{b_{12}}$)	0.039, 0.047	2.2	0.2	0.052, 0.045	2.0	0.1

			PR-EoS				RKS-EoS			
ternary mixture	number of ternary data	mixing and combining rule	values of adjusted parameters	σ^R_p/%	σ^R_{y1}/%	σ^R_{y2}/%	values of adjusted parameters	σ^R_p/%	$\sigma^R_{y_1}$/%	$\sigma^R_{y_2}$/%
hydrogen sulfide (1) + hexane (2) + pentadecane (3)	15	R0		4.8	4.1	9.7		5.9	4.9	8.8
		R1(δ_{12})	0.060				0.070			
		(δ_{13})	−0.016	4.2	2.2	10.	0.000	4.6	1.9	7.8
		(δ_{23})	0.000				0.000			
		R2($\delta_{a_{12}}$,$\delta_{b_{12}}$)	0.088, 0.048				0.096, 0.042			
		($\delta_{a_{13}}$,$\delta_{b_{13}}$)	0.039, 0.047	3.8	2.0	6.2	0.052, 0.045	4.2	1.8	4.9
		($\delta_{a_{23}}$,$\delta_{b_{23}}$)	0.000, 0.000				0.000, 0.000			

[a] $\sigma^R_u = 100[\Sigma((u_{j,\mathrm{exp}} - u_{j,\mathrm{cal}})/u_{j,\mathrm{exp}})^2/(n - k)]^{1/2}$ (k = number of model parameters).

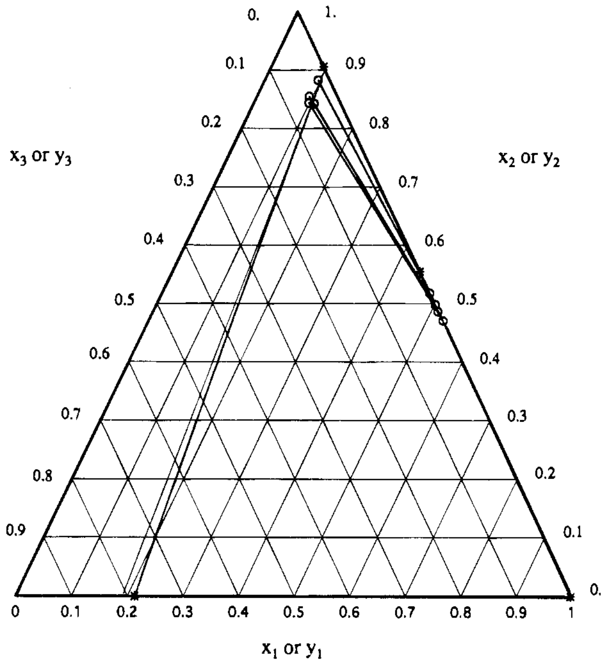

Figure 6. Hydrogen sulfide mole fraction as a function of hexane and pentadecane mole fractions in the hydrogen sulfide (1) + hexane (2) + pentadecane (3) system at 424.5 K (○) and 1.53 MPa; (*) interpolated value from binary data; (light line) calculated results with the RKS-EoS and binary interaction parameter (R1 rule) given in Table 8; (dark line) calculated results with the RKS-EoS and binary interaction parameters (R2 rule) given in Table 8.

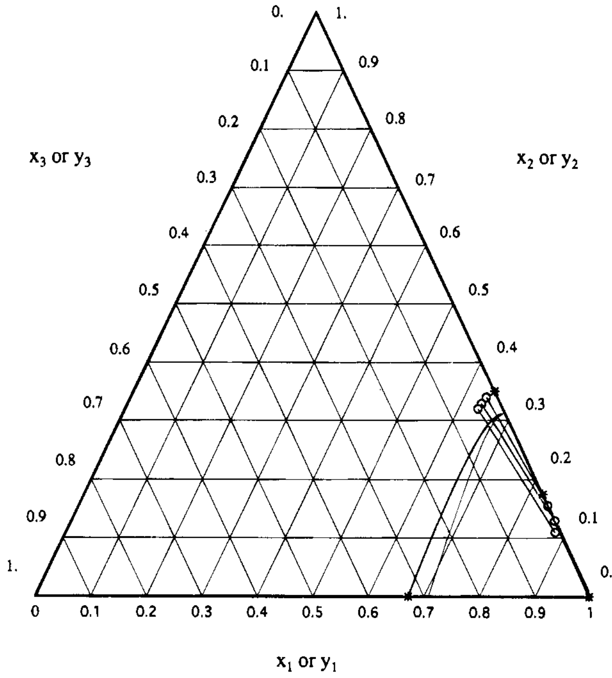

Figure 7. Hydrogen sulfide mole fraction as a function of hexane and pentadecane mole fractions in the hydrogen sulfide (1) + hexane (2) + pentadecane (3) system at 424.5 K (○) and 7.50 MPa; (*) interpolated value from binary data; (light line) calculated results with the RKS-EoS and binary interaction parameter (R1 rule) given in Table 8; (dark line) calculated results with the RKS-EoS and binary interaction parameters (R2 rule) given in Table 8.

High-pressure data from Feng and Mather (*7–9*) have been treated using the Peng–Robinson equation of state and rule R1 to test the consistency with our data. For hydrogen sulfide + dodecane, + hexadecane, and + eicosane, respectively, optimal *kij* values of 0.000,−0.015,−0.038 have been found. The infinite dilution Henry's constants which have then been deduced are, respectively, 7.9, 7.0, and 6.4 at 423 K. At the same temperature for pentadecane + hydrogen sulfide our data lead to about 7 MPa.

The ternary system is slightly better represented using rule R1 instead of rule R0. The binary interaction parameter for hexane + pentadecane has been taken to 0 as no VLE data are available for this system in our temperature–pressure range. Figures 6 and 7 are examples of ternary diagrams comparing experimental results to calculations.

Use of more complex combining rules such as those from Panagiotopoulos (*10*) or Huron-Vidal (*11*) have no positive

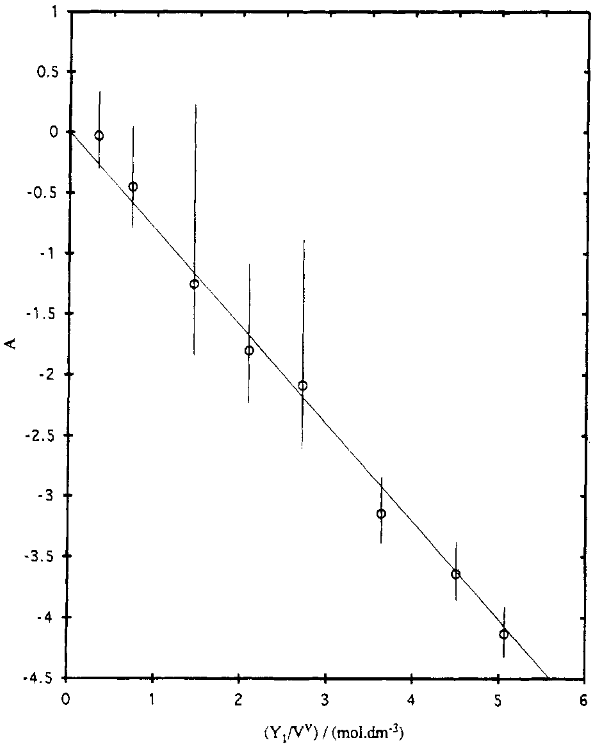

Figure 8. A as a function of y_1/V^v in the hydrogen sulfide (1) + pentadecane (2) system at 423 K (○).

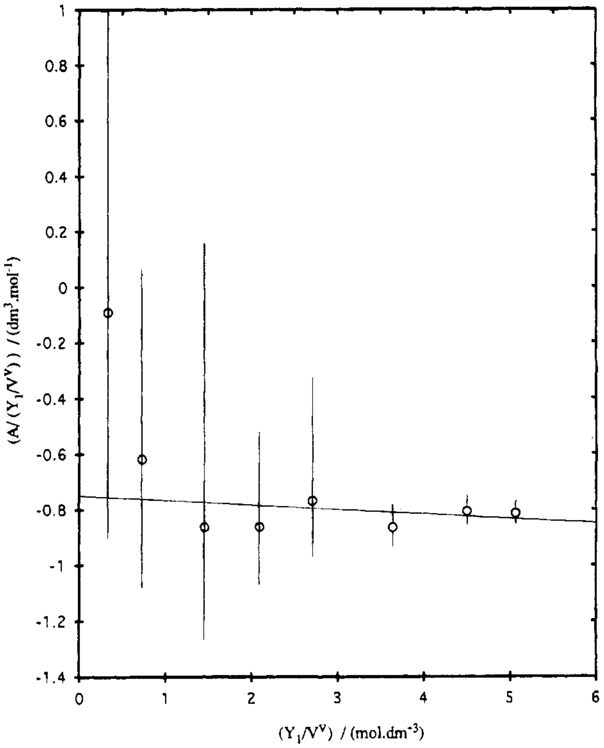

Figure 9. $A/(y_1/V^v)$ as a function of y_1/V^v in the hydrogen sulfide (1) + pentadecane (2) system at 423 K (○).

effect on the representation quality. The same conclusion is made with other equations of state such as the Patel–Teja EoS (*12*) or the Trebble–Bishnoi–Salim EoS (*13*). Furthermore, in some cases we would be confronted with the Michelsen–Kistenmacher syndrome (*14*).

Prausnitz–Keeler Test

It is possible to demonstrate (*15*) that the logarithm of the fugacity coefficient of the less volatile component can be obtained both from the experimental results, neglecting the Poynting correction, the activity coefficient in the liquid phase, and the fugacity coefficient in the reference state, and from a virial development reduced to two terms, neglecting smaller terms:

$$A = \ln(x_2P_2^SZ^v/y_2P) = 2y_1/V^v\left(B_{12} + \frac{3/4y_1}{V^vC_{112}}\right) \qquad (2)$$

where 2 is the index of the less volatile component, P_2^S is its saturation pressure, P is the total pressure, Z^v is the compressibility factor, V^v is the molar volume of the vapor phase, and B_{12} and C_{112} are the second and third virial coefficients. The straight line in Figure 8 plots A against y_1/V^v and has a slope of $2B_{12}$. We find $B_{12} = -0.40 \pm 0.1$ dm³·mol⁻¹. The Tsonopoulos (*16*) correlation gives −0.81 dm³·mol⁻¹ while a direct calculation through the Peng–Robinson equation of state leads to $B_{12} = -0.66$ dm³·mol⁻¹. The third virial coefficient can sometimes be estimated (*17*), but in this work the pressure range is not large enough and the influence of the third virial coefficient is negligible on $A/(y_1/V^v)$ as a function of y_1/V^v (see Figure 9).

Acknowledgment

We are grateful to Dr. Montel and Dr. Desgranchamps for helpful discussion. We thank C. LAFEUIL we took part in the measurements.

Appendix

Equations of State (EoS) for Pure Substances. The general form is given by the expression

$$P = \frac{RT}{v - b} - \frac{a[T]}{v(v + b) + c(v - b)} \qquad (A1)$$

with

$$a[T] = (\Omega_aR^2T_c^{\,2}/P_c)\alpha(T_r) \qquad (A2)$$

$$b = \Omega_bRT_c/P_c \qquad (A3)$$

$$c = \Omega_cRT_c/P_c \qquad (A4)$$

Soave Equation of State (RKS-EoS). There are three parameters, T_c, P_c, and ω (acentric factor), taken from the literature (see Table 7).

$$\Omega_a = 0.427\,47 \qquad (A5)$$

$$\Omega_b = 0.0866 \qquad (A6)$$

$$\Omega_c = 0 \qquad (A7)$$

$$\alpha(T_r) = [1 + m(1 - T_r^{\,1/2})]^2 \qquad (A8)$$

$$m = 0.48508 + 1.55171\omega - 0.15613\omega^2 \qquad (A9)$$

Peng–Robinson Equation of State (PR-EoS). There are three parameters, T_c, P_c, and ω taken from the literature (see Table 7).

$$\Omega_a = 0.457\,24 \qquad (A10)$$

$$\Omega_b = 0.0778 \qquad (A11)$$

$$\Omega_c = \Omega_b \qquad (A12)$$

$$\alpha(T_r) = [1 + m(1 - T_r^{\,1/2})]^2 \qquad (A13)$$

$$m = 0.37464 + 1.54226\omega - 0.26992\omega^2 \qquad (A14)$$

Mixing and Combining Rules.

RO: mixing rules

$$a = \sum_i \sum_j a_{ij} x_i x_j \tag{A15}$$

$$b = \sum_i b_i x_i \tag{A16}$$

combining rule

$$a_{ij} = (a_i a_j)^{1/2} \tag{A17}$$

R1: mixing rules

$$a = \text{eq A15}$$

$$b = \text{eq A16}$$

combining rule

$$a_{ij} = (a_i a_j)^{1/2}(1 - \delta_{ij}) \tag{A18}$$

R1T: mixing rules

$$a = \text{eq A15}$$

$$b = \text{eq A16}$$

combining rule

$$a_{ij} = (a_i a_j)^{1/2}(1 - \delta_{ij} - \delta'_{ij}/T) \tag{A19}$$

R2T: mixing rules

$$a = \text{eq A15}$$

$$b = \sum_i \sum_j b_{ij} x_i x_j \tag{A20}$$

combining rules

$$a = \text{eq A18}$$

$$b_{ij} = \frac{b_i + b_j}{2}(1 - \delta_{b_{ij}}) \tag{A21}$$

Literature Cited

(1) Figuière, P.; Hom, J. F.; Laugier, S.; Renon, H.; Richon, D.; Szwarc, H. *AIChE J.* **1980**, *26*, 872.
(2) Laugier, S. Thesis Dissertation, Ecole Nationale Supérieure des Mines, Paris, 1982.
(3) Laugier, S.; Richon, D. *Rev. Sci. Instrum.* **1986**, *57*, 469.
(4) Soave, G. *Chem. Eng. Sci.* **1972**, *27*, 1197.
(5) Peng, D. Y.; Robinson, D. B. *Ind. Eng. Chem. Fundam.* **1976**, *15*, 59.
(6) Reid, R. C.; Prausnitz, J. M.; Sherwood, T. K. *The properties of gases and liquids*; McGraw-Hill Book Co. London, 1977.
(7) Feng, G. X.; Mather, A. E. *Fluid Phase Equilib.* **1993**, *87*, 341.
(8) Feng, G. X.; Mather, A. E. *Can. J. Chem. Eng.* **1993**, *71*, 327.
(9) Feng, G. X.; Mather, A. E. *J. Chem. Eng. Data* **1992**, *37*, 412.
(10) Panagiotopoulos, A. Z.; Reid, R. C.; Prausnitz, J. M. *ACS Symp. Ser.* **1986**, *300*, 571.
(11) Huron, H.; Vidal, J. *Fluid Phase Equilib.* **1979**, *3*, 255.
(12) Patel, N. C.; Teja, A. S. *Chem. Eng. Sci.* **1982**, *37*, 463.
(13) Trebble, M. A.; Bishnoï, P. R. *Fluid Phase Equilib.* **1986**, *29*, 465.
(14) Michelsen, M. I.; Kistenmacher, H. *Fluid Phase Equilib.* **1990**, *58*, 229.
(15) Prausnitz, J. M.; Keeler, R. N. *AIChE J.* **1961**, *7*, 399.
(16) Tsonopoulos, C. *AIChE J.* **1974**, *20*, 263.
(17) Renon, H.; Laugier, S.; Schwartzentruber, J.; Richon, D. *Fluid Phase Equilib.* **1989**, *51*, 285.

Received for review April 19, 1994. Accepted August 3, 1994.[⊗] We are grateful to ELF for financial support.

JE9400724

[⊗] Abstract published in *Advance ACS Abstracts,* November 15, 1994.